ELECTRONIC SUPPLEMENTARY INFORMATIONS

A new and facile strategy for the one-pot fabrication of luminescent gold nanoclusters and its prospective application

Tanur Sinha and M. Ahmaruzzaman*

Department of Chemistry, National Institute of Technology Silchar, Silchar 788010, India

E-mail: md_a2002@rediffmail.com (M. Ahmaruzzaman); Tel.: +91-3842242915; Fax: +91-3842224797.

S1 *Evaluation of the photocatalytic activity of the synthesized Au NCs:*

The spectra of the photocatalytic activity of both the dye solution under dark condition is shown in (Fig. S1(a) and (c)). While the controlled absorption spectra of both the dyes degradation in absence of Au NCs is represented by (Fig. S1 (b) and (d)).

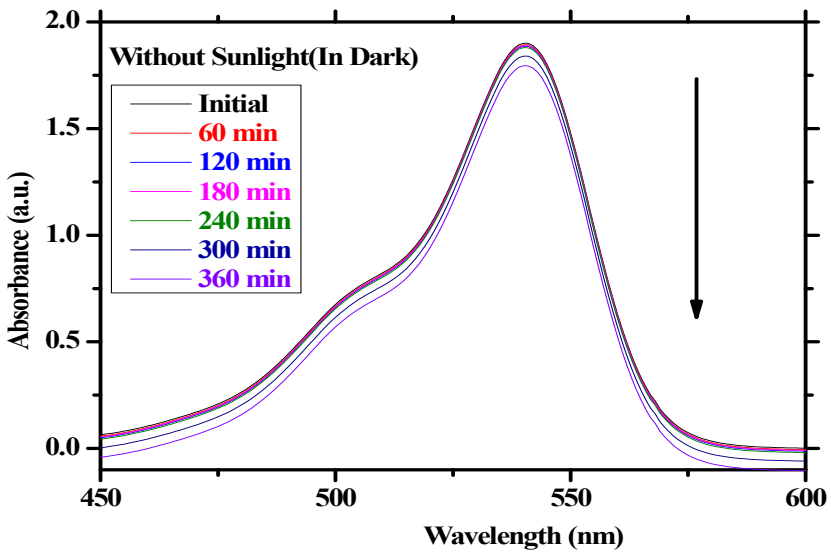

Fig. S1 (a) represented the absorption spectra for photocatalytic degradation of RB under dark reaction conditions.

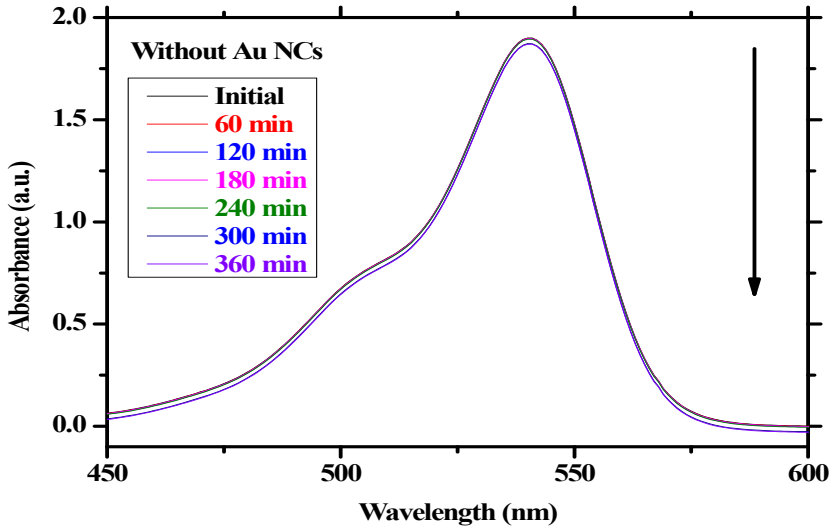

Fig. S1 (b) represented the absorption spectra for photocatalytic degradation of RB in absence of Au NCs.

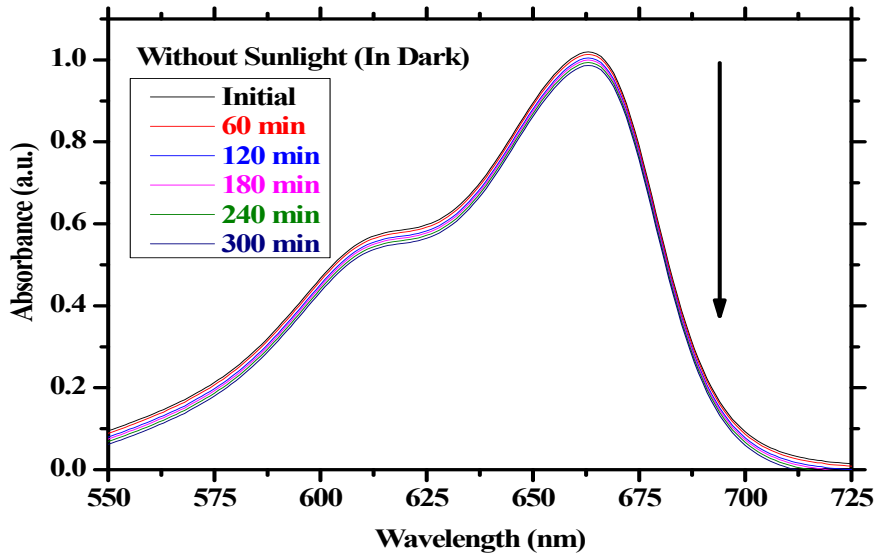

Fig. S1 (c) represented the absorption spectra for photocatalytic degradation of MB under dark reaction conditions.

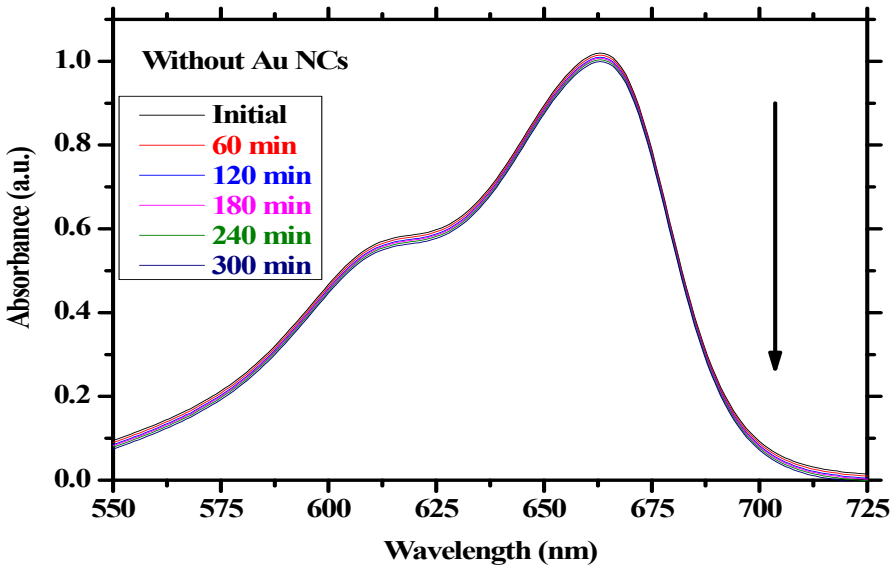

Fig. S1 (d) represented the absorption spectra for photocatalytic degradation of MB in absence of Au NCs.

S2 Photostability of the Au NCs as catalyst:

(Fig. S2 (a) and (d)) represented the TEM image of the spent catalyst recovered after 3 cycles of photodegradation of RB and MB respectively. The TEM images revealed that the clusters morphology is almost similar instead the cluster morphology has been slightly increased (9-11nm) in case of RB (as revealed from the histogram in the inset of Fig. S2 (a)) and (10-12 nm) in case of MB (revealed from the histogram depicted in the inset of Fig. S2 (d)).

The HRTEM images (Fig. S2 (b) and (e)) showed the fringe spacing to be consistent with (111) lattice plane of fcc Au NCs with 0.26 nm in both cases. The SAED pattern (Fig. S2 (c) and (f)) revealed the polycrystalline nature.

The results of the recyclability test for RB and MB are respectively shown in (Fig. S2 (g) and (h)). Thus, it is relevant that the Au NCs exhibits excellent photostability under solar irradiation even after 3 cycles of recovery with unaltered morphology of the catalyst.

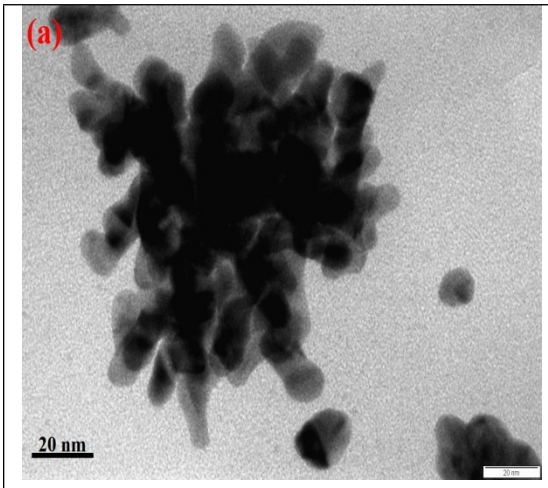
(a)
20 nm

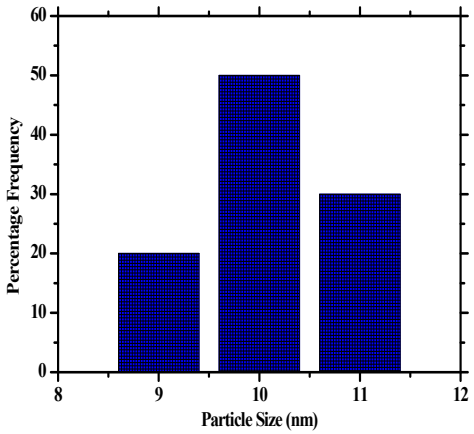
Percentage Frequency
Particle Size (nm)
0
10
20
30
40
50
60
8
9
10
11
12

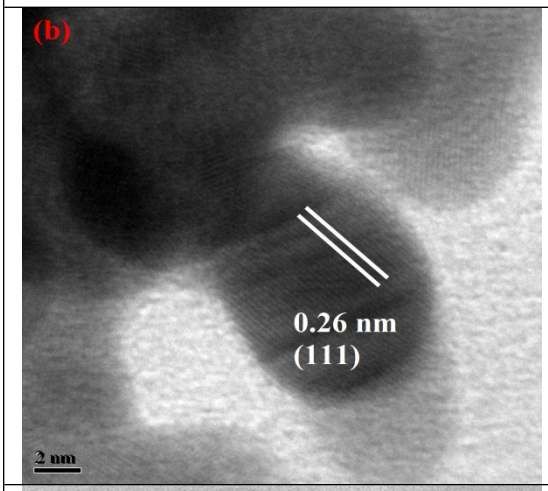
(b)
0.26 nm
(111)
2 nm

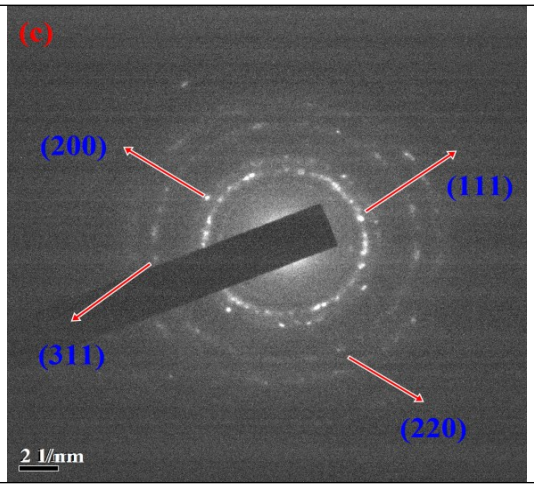
(c)
(200)
(111)
(311)
(220)
2 1/nm

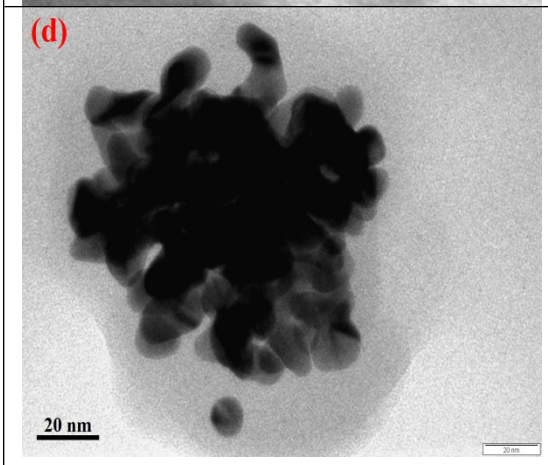
(d)
20 nm

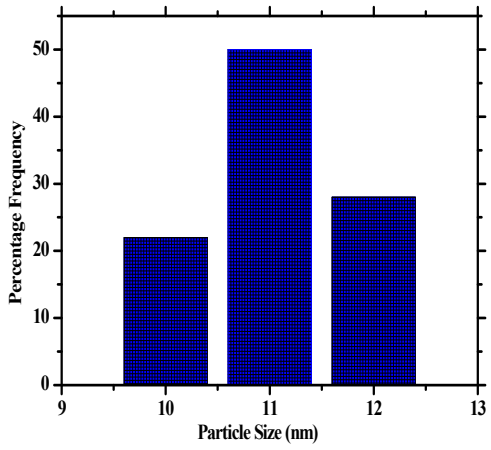
Percentage Frequency
Particle Size (nm)
0
10
20
30
40
50
9
10
11
12
13

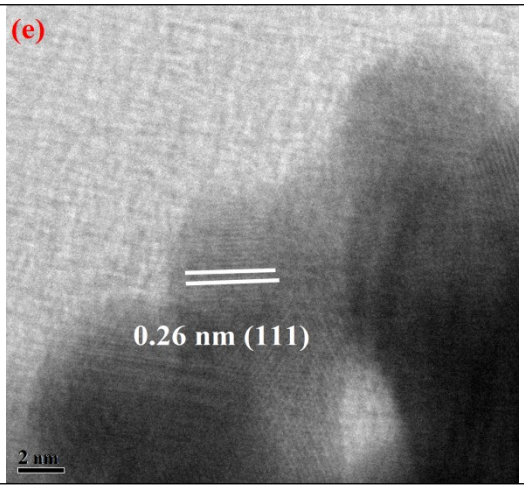

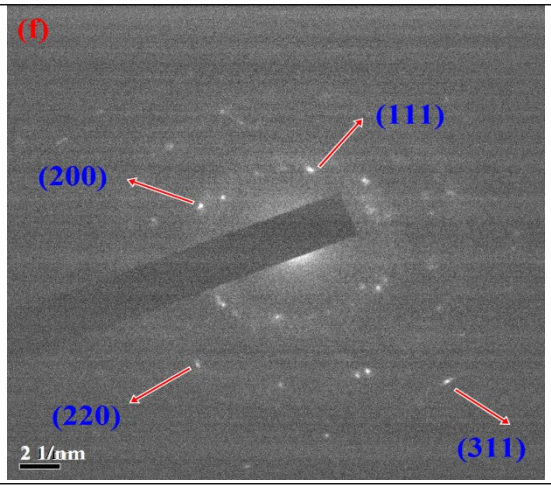

(g)

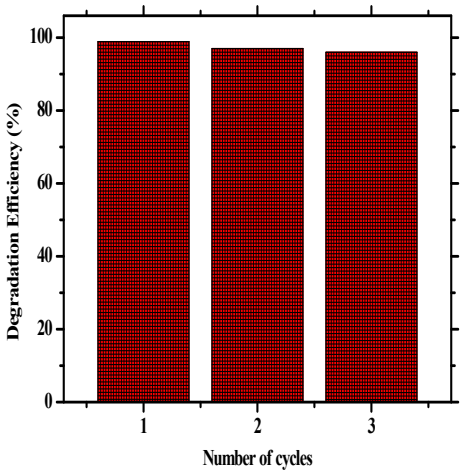

(h)

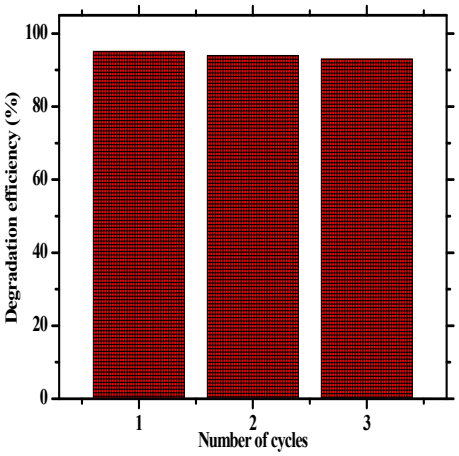

(Fig. S2(a) and (d)) corresponded to the TEM images (inset size distribution) of the spent Au NCs catalyst recovered after 3 cycles of photodegradation of RB and MB respectively. The SAED pattern of (Fig. S2 (a) and (d)) are shown in (Fig. S2 (c) and (f)) respectively and (Fig. S2 (b) and (e)) are the magnified images of (Fig. S2 (a) and (d)) respectively. Recyclability tests of Au NCs catalyst for degradation of RB and MB are depicted in (Fig. S2 (g) and (h)) respectively.

S3 Identification of the intermediate products of dye degradation:

The intermediates generated during the degradation process were analyzed using LC-MS technique and were identified by comparison with commercial standards and by interpretation of their fragment ions in the mass spectra.

Fig. S3(a) displayed the LC-MS of RB dye solution with Au NCs initially. The figure depicted a prominent mass signal at m/z=1022 which is very close to the formula mass of RB dye.

Noticeably, no mass signals corresponding to the formula of degradation products were found. Fig. S3(b) showed the LC-MS of RB dye solution with Au NCs after 180 min. The experimental data indicated that the wastewater was significantly decolorized or degraded at the end of 180 min irradiation. Here, it was observed that the signal at m/z=1022 was weakened and multiple signals corresponding to the reaction intermediates (degraded products) were found. Many peaks of different intensities were observed which showed the variation in composition and concentration of the degradation products. The molecular structures of the possible degradation products from fragmentation of the main skeleton of RB which have the oxy groups in their rings were represented in Fig. S3(c). It is believed that the formations of these reaction intermediates are very important to determine the degree of degradation of the organic compounds to complete the mineralization process [1].

Fig. S3(d) depicted the LC-MS of MB dye solution with Au NCs initially. The figure clearly displayed a prominent peak at m/z =284 which is very close to the formula mass of MB dye and no other signals were found. Fig. S3(e) represented the LC-MS of MB dye solution with Au NCs after 145 min (complete degradation). Here, it was found that the signal at m/z = 284 is weakened and multiple mass signals corresponding to various degradation products have been appeared. The molecular structures of the degradation products from fragmentation of the main skeleton of MB dye were shown in Fig. S3(f). It was supposed that the formation of

the degradation products took place by cleavage of one or more of the methyl groups on the amine group. For example, the formation of azure A, B and C and thionin (Fig. S3(f)) through the demethylation cleavage during the photocatalytic degradation has been observed [2]. It is then predicted from the LC-MS (Fig. S3(e)) that the Azure C undergone fragmentation to give intermediate degraded products at m/z =186, 142 and 123 (Fig. S3(g)). Henceforth, it could be concluded that the synthesized Au NCs showed marvellous photocatalytic activity because of high surface area to volume ratio, which provided maximum exposure for the reactant to the active surface. As a whole, the photodegradation of dyes using synthesized NPs in the visible light can be explained because of the excitation of surface plasmon resonance, which is actually the oscillation of charge density that can propagate at the interface between the metal and the dielectric medium.

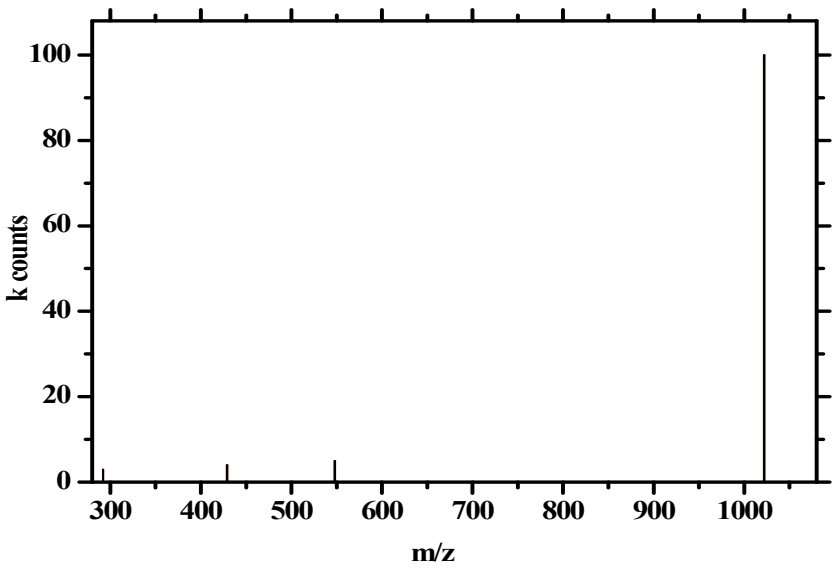

Fig. S3 (a) represented the LC-MS of RB dye solution with Au NCs after 0 minutes.

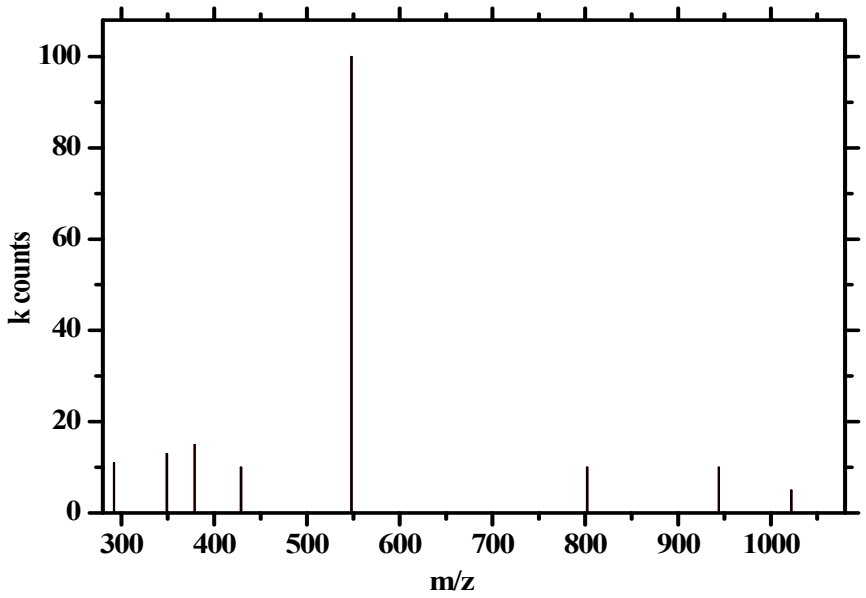

Fig. S3 (b) represented the LC-MS of RB dye solution with Au NCs after 180 minutes.

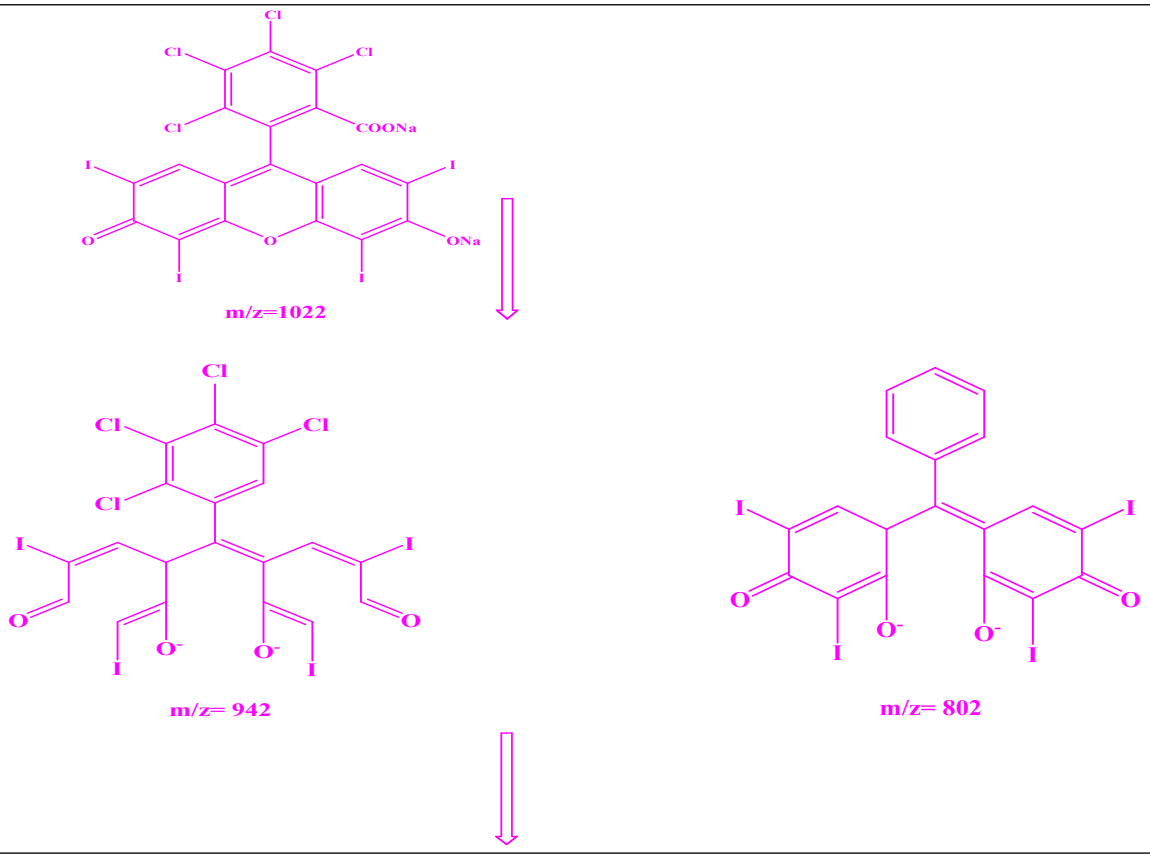

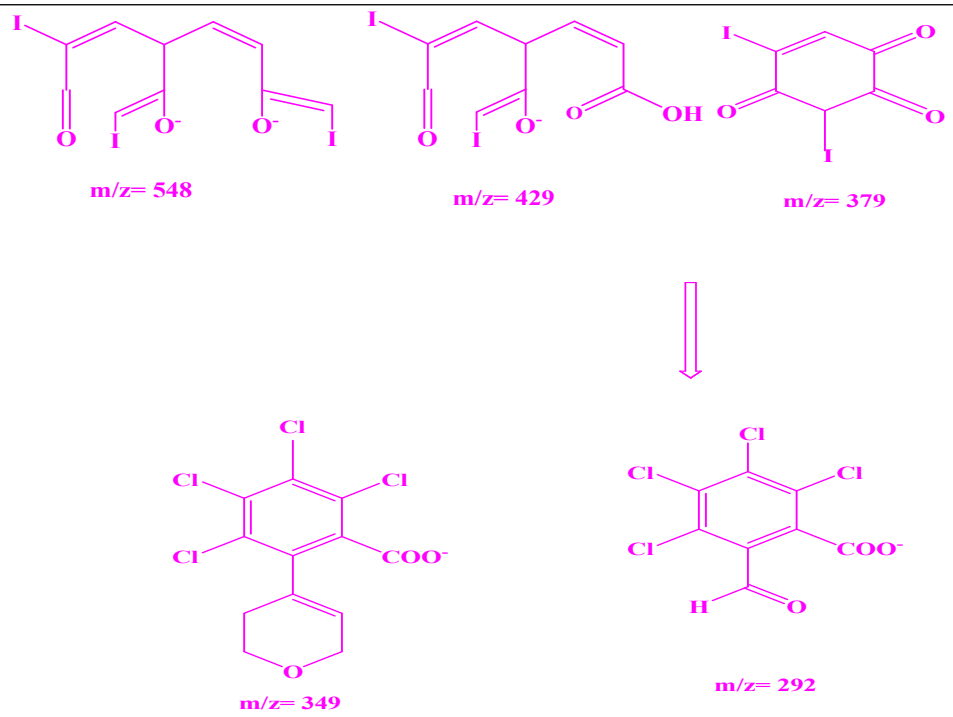

Fig.S3(c) depicted the molecular structures of the possible reaction intermediates from fragmentation of the main skeleton of RB dye.

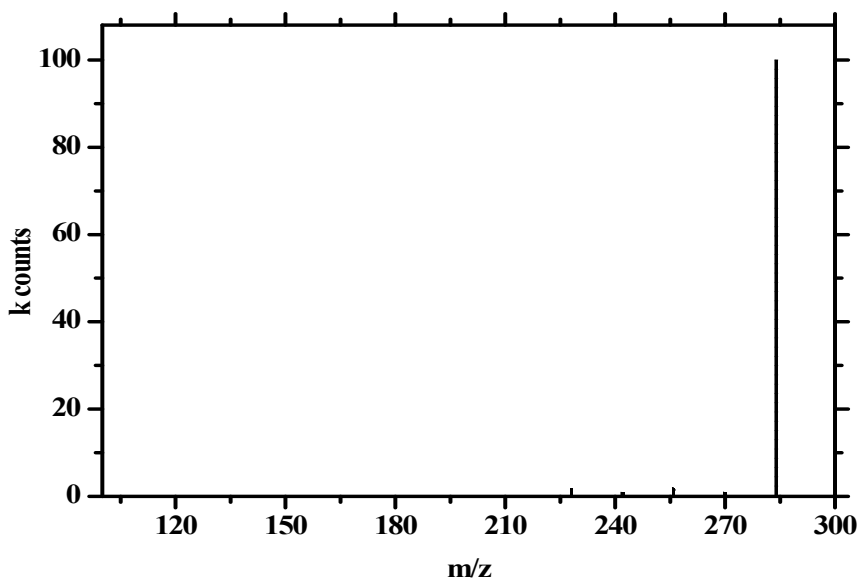

Fig. S3 (d) showed the LC-MS of MB dye solution with Au NCs after 0 minutes.

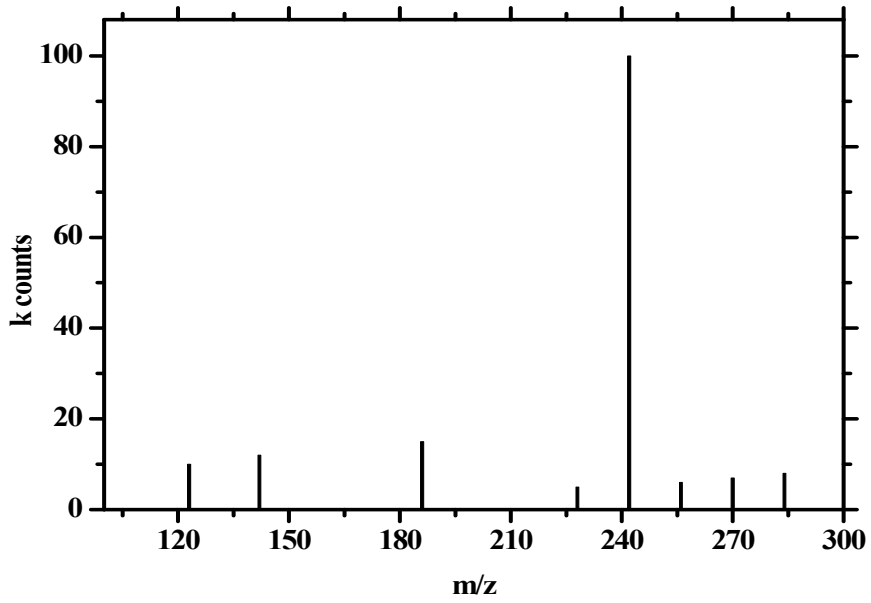

Fig. S3 (e) showed the LC-MS of MB dye solution with Au NCs after 145 minutes.

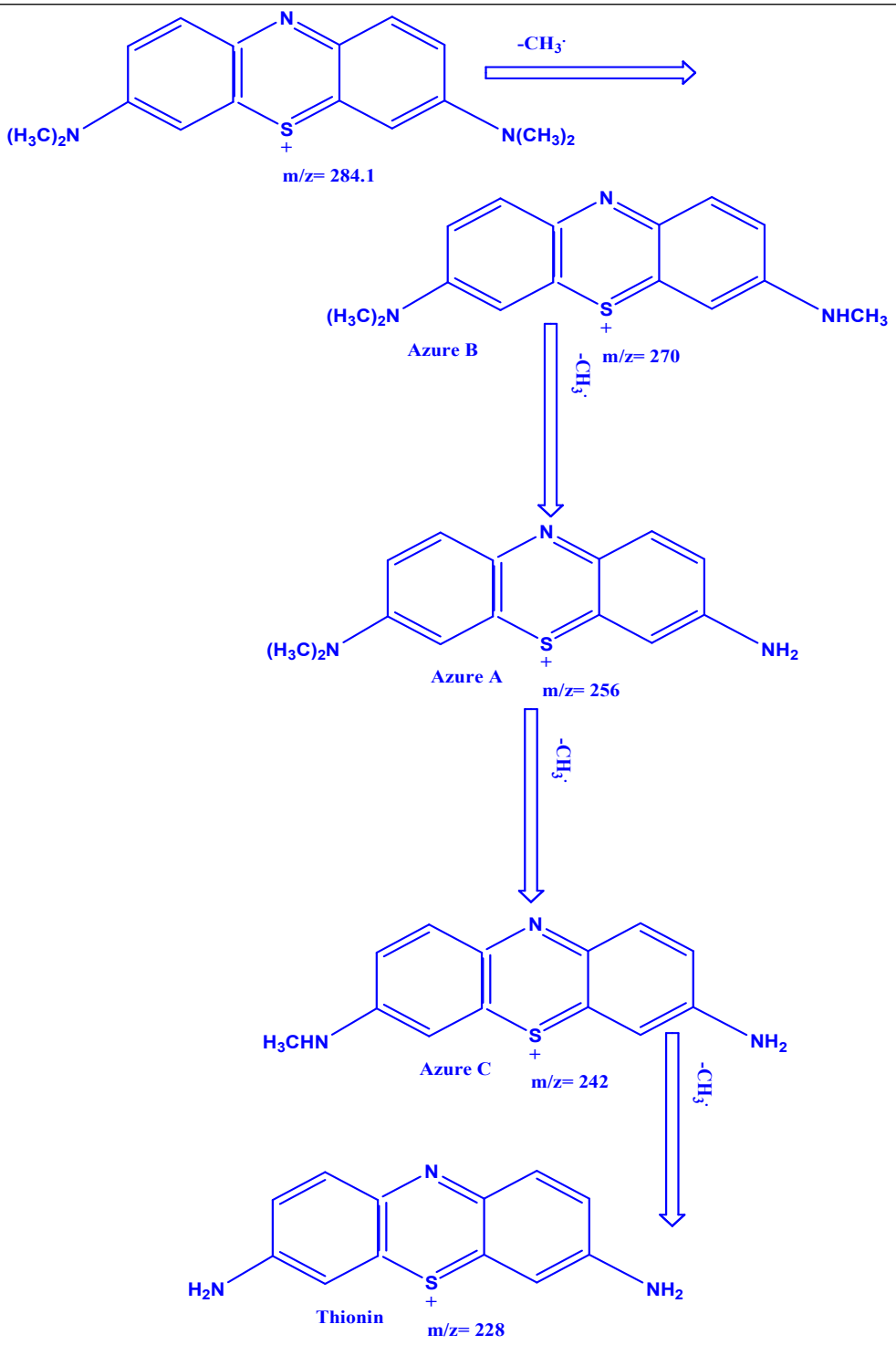

Fig. S3 (f) depicted the molecular structures of the possible reaction intermediates from fragmentation of the main skeleton of MB dye.

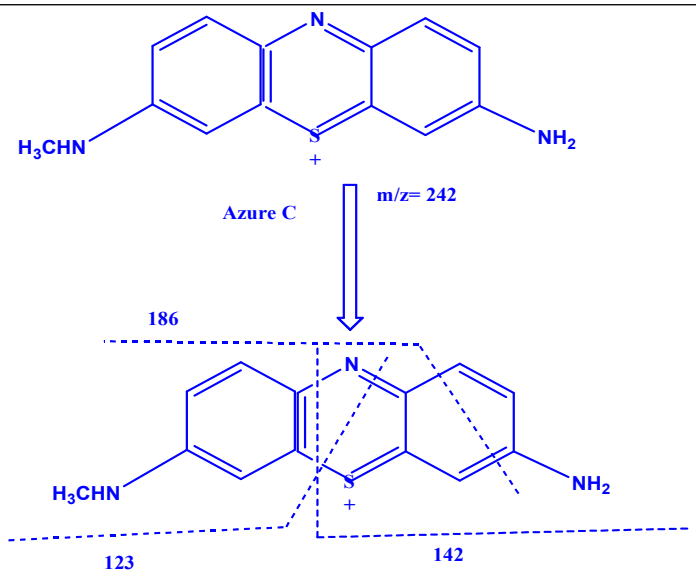

Fig. S3 (g) represented the mass spectra of MB intermediate degradation product ion at m/z = 242.

S4.Catalytic reduction of 4-NP to 4-AP employing Au NCs as catalyst in aqueous medium:

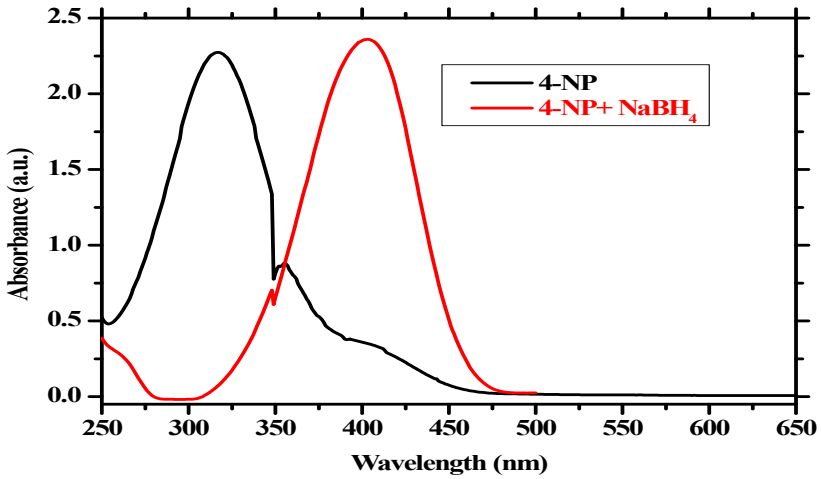

Fig. S4(a) represented the absorbance spectra of 4-NP and 4-NP + $NaBH_4$ in aqueous medium.

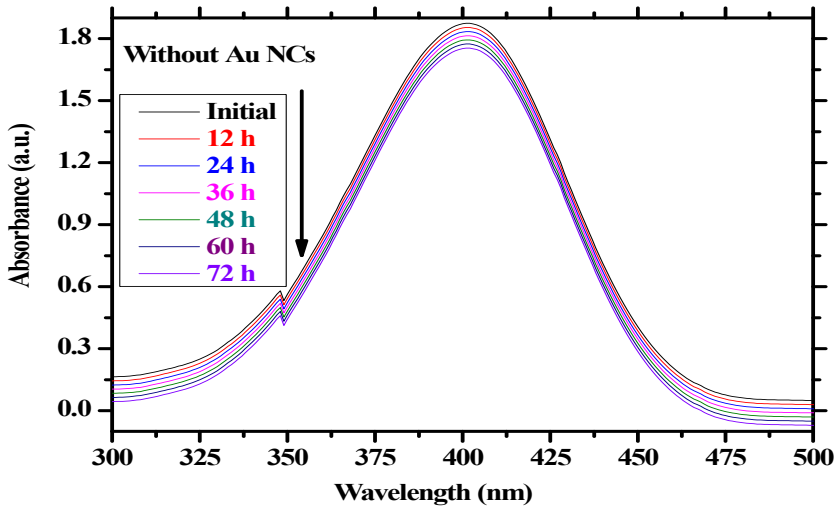

Fig. S4 (b) represented the absorption spectra for the reduction of 4-NP by $NaBH_4$ in aqueous medium in absence of any catalyst.

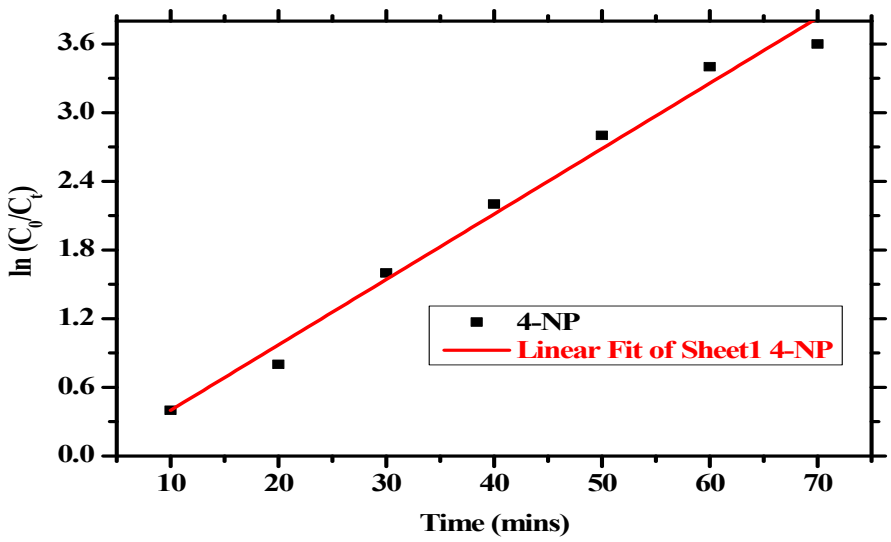

Fig. S4(c) depicted the Plot of ln (C_0/C_t) versus time required for the reduction of 4-NP using Au NCs as catalyst in presence of $NaBH_4$ in aqueous medium.

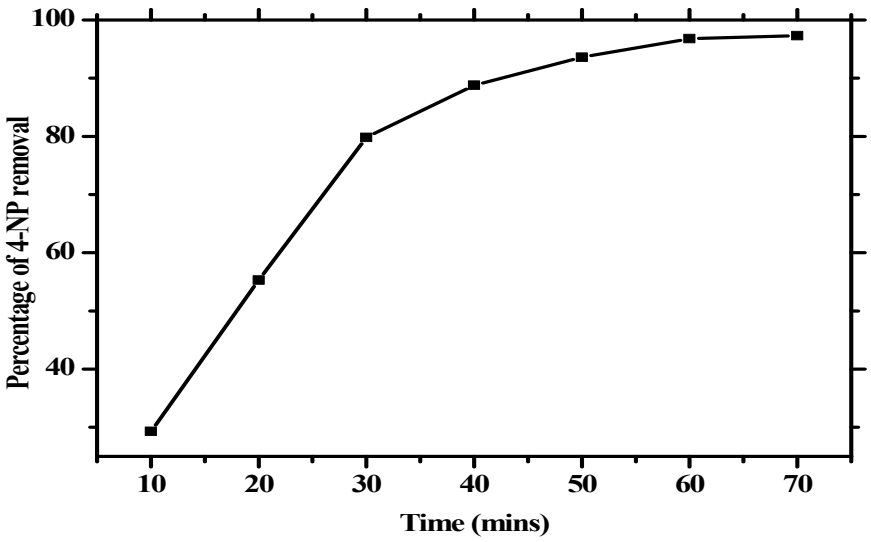

Fig. S4 (d) represented the degradation capacity of the manufactured NCs for removal of 4-NP.

S5 Mechanism of reduction of 4-NP to 4-AP:

The mechanism of reduction of 4-NP to 4-AP can be illustrated in terms of Langmuir Hinshelwood model (Scheme 1) [3].

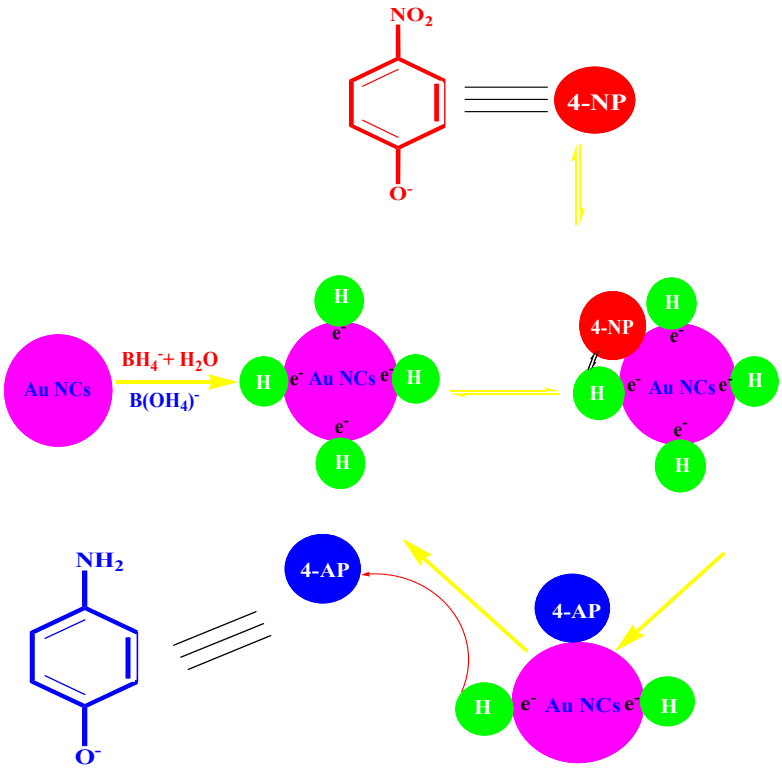

Scheme 1. Mechanism of reduction of 4-NP to 4-AP

Initially on the surface on the surface of Au NCs, the adsorption of boride ions and transfer of a surface-H specie takes place. Simultaneously, 4-NP are also adsorbed on the cluster surface. Finally, the H atom at the Au NCs surface react with 4-NP to yield the product 4-AP. 4-AP then undergoes desorption. Thus, making the catalyst surface free and the catalytic cycle can begin again. Henceforth, the reduction reaction could be summarized by the following equation:

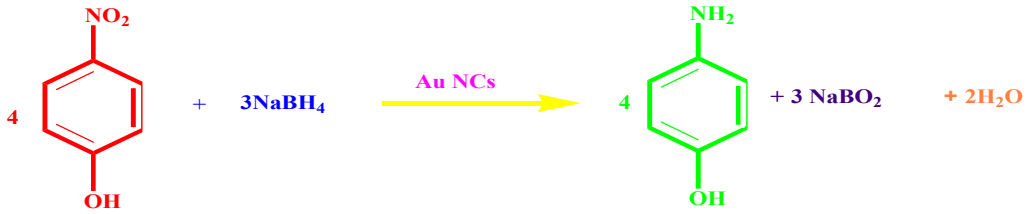

4-NP **4-AP**

LIST OF TABLES:

Table T1. EDAX elemental analysis of Au NCs.

S.NO	Sample name	Weight %	Atomic %	keV
1.	Au NCs	Au = 87	Au = 90	Au = 2, 8.5, 9.6
		Cu = 3.2	Cu = 2.15	Cu = 8 , 9
		Fe = 1.62	Fe = 1.23	Fe = 7
		K = 4	K = 2.7	K = 3.6
		S = 2.74	S = 2.63	S = 2.3
		P = 1.11	P = 0.97	P = 2
		Si = 0.33	Si = 0.32	Si = 1.8

Table T2. FTIR spectra of AvL extract and fabricated Au NCs.

Samples	FTIR bands (cm^{-1})						
	ν_{O-H} with ν_{N-H}	ν_{S-H}	$\nu_{C=O}$ of amide	ν_{N-H} bending of amide/ ν_{C-H} in aromatic hydrocarbon	ν_{C-O-H} bending of carboxylic acid/ in plane ν_{O-H} bending	ν_{C-H} bending aromatic hydrocarbon	ν_{N-H} wagging /out of plane ν_{O-H} bending
AcL extract	3440	2550	1611	1358	1012	719	550
Au NCs	3452	-	1625	1386	998	-	585

Table T3. Inhibitory action of control, AcL extracts and fabricated Au NCs against *Escherichia coli bacteria.*

Bacterial Species	Inhibition Zone (mm)		
	Control (Tetracycline)	AcL Extract (200 µg/ml)	Au NCs+ Tetracycline (200 µg/ml)
Escherichia coli	20	6	30

REFERENCES:

1. S. Ameen, H.K.Seo, M.S.Akhtar, H.S.Shin, Novel graphene/polyaniline nanocomposites and its photocatalytic activity toward the degradation of rose Bengal dye, Chem. Eng. J., 2012, 210, 220-228.

2. M. A. Rauf, M.A. Meetani, A. Khaleel, A. Ahmed, Photocatalytic degradation of Methylene Blue using a mixed catalyst and product analysis by LC/MS. Chem. Eng. J. 2010, 157, 373-378.

3. S. Wunder, F. Polzer, Y. Lu, Y. Mei, M. Ballauff, Kinetic Analysis of Catalytic Reduction of 4-Nitrophenol by Metallic Nanoparticles Immobilized in Spherical Polyelectrolyte Brushes, J. Phys. Chem. C., 114 (2010) 8814–8820.